PROCEEDINGS OF SCIENCE

# Measurement of photon production in proton-proton collisions at $\sqrt{s}$ = 13 TeV with the ATLAS detector

PoS(EPS-HEP2019)648

ATL-PHYS-PROC-2019-135
17 October 2019

**Josu Cantero***, **on behalf of ATLAS Collaboration**
*Oklahoma State University (OSU), Stillwater, USA*
*E-mail:* jcantero@cern.ch

The production of prompt photons in proton-proton collisions at the LHC provides a testing ground for perturbative QCD with a hard colourless probe. Since the dominant production mechanism in proton–proton collisions proceeds via the $qg \to g\gamma$ process, measurements of prompt-photon and photon plus jet production are sensitive at leading order to the gluon density in the proton. This contribution presents the latest ATLAS measurements of the ratio of the cross sections for inclusive isolated-photon production at centre-of-mass energies of 13 and 8 TeV, the measurements of isolated-photon plus jet cross sections at $\sqrt{s}$ = 13 TeV using a dataset with an integrated luminosity of 3.2 fb$^{-1}$ and the differential cross section for isolated-photon production measured at $\sqrt{s}$ = 13 TeV using an integrated luminosity of 36.1 fb$^{-1}$. The measurements are compared to next-to-leading-order QCD as well as to next-to-next-to-leading-order QCD calculations.

*European Physical Society Conference on High Energy Physics - EPS-HEP2019 -
10-17 July, 2019
Ghent, Belgium*

*Speaker.

## 1. Introduction

The production of prompt photons in proton–proton ($pp$) collisions at the LHC, $pp \to \gamma$+X, provides a testing ground for perturbative QCD (pQCD) with a hard colourless probe. All photons produced in $pp$ collisions that are not products of the hadron decays are considered as "prompt". Two processes contribute to prompt-photon production: the direct process, in which the photon originates directly from the hard interaction, and the fragmentation process, in which the photon is emitted in the fragmentation of a high transverse momentum ($p_{\mathrm{T}}$) parton [1, 2]. Measurements of inclusive prompt-photon production were used recently to investigate novel approaches to the description of parton radiation [3] and the importance of resummation of threshold logarithms in QCD and of the electroweak corrections [4]. Since the dominant production mechanism in $pp$ collisions proceeds via the $qg \to g\gamma$ process, measurements of prompt-photon and photon production in association with jets are sensitive to the gluon density in the proton at Leading Order (LO) [5]. Therefore, new measurements of prompt-photon production are expected to further constrain the gluon density in the proton.
In the ATLAS experiment [6], photons are identified as clusters of energy in the electromagnetic (EM) calorimeter in pseudorapidity regions of $|\eta| < 1.37$ (central) and $1.56 < |\eta| < 2.37$ (forward) [7]. Additional identification requirements, aimed at the removal of contribution of photons from decays of energetic $\pi^0$ and $\eta$ mesons inside jets, are applied to the lateral and longitudinal energy profiles of the EM shower in the calorimeter [8]. Photon candidates are required to be isolated, which is ensured by applying cuts on the total transverse energy in a cone of R = 0.4 centered around the photon direction: $E_{\mathrm{T}}^{\mathrm{iso}} < 0.0042\times E_{\mathrm{T}}^{\gamma}$ + 4.8 GeV where $E_{\mathrm{T}}^{\gamma}$ is the photon transverse energy. To remove the contribution coming from pileup, the calorimeter isolation is corrected using the jet area method [9]. Remaining non-negligible background is evaluated by using a data-driven method based on signal-suppressed control regions [10].

## 2. Ratio of cross sections for inclusive isolated-photon at $\sqrt{s}$ = 13 and 8 TeV

The measurements of ratios of cross sections [11] are based on the measurements presented in previous ATLAS publications [1, 2]. The impact of the experimental systematic uncertainties and theoretical uncertainties on the ratio of the cross sections is reduced, allowing a more precise comparison between data and theory. This is achieved by accounting for inter-$\sqrt{s}$ correlations in the experimental systematic uncertainties affecting the measurements and in the uncertainties of the theory predictions. The measurement of the ratio covers the range $E_{\mathrm{T}}^{\gamma} > 125$ GeV and is performed separately in the four regions of $|\eta^{\gamma}|$, namely $|\eta^{\gamma}| < 0.6$, $0.6 < |\eta^{\gamma}| < 1.37$, $1.56 < |\eta^{\gamma}| < 1.81$ and $1.81 < |\eta^{\gamma}| < 2.37$.
The measured 13-to-8 TeV inclusive isolated-photon cross section ratio, $R^{\gamma}_{13/8}$, as a function of $E_{\mathrm{T}}^{\gamma}$ in different regions of $|\eta^{\gamma}|$, together with the NLO QCD prediction estimated by JETPHOX [12], are shown in Figure 1. Even though there is a tendency for the predictions to underestimate the data, the measurements and the theory are consistent within the uncertainties. The overall level of agreement between data and the NLO QCD predictions within the uncertainties validates the description of the evolution of isolated-photon production in $pp$ collisions with the centre-of-mass energy.

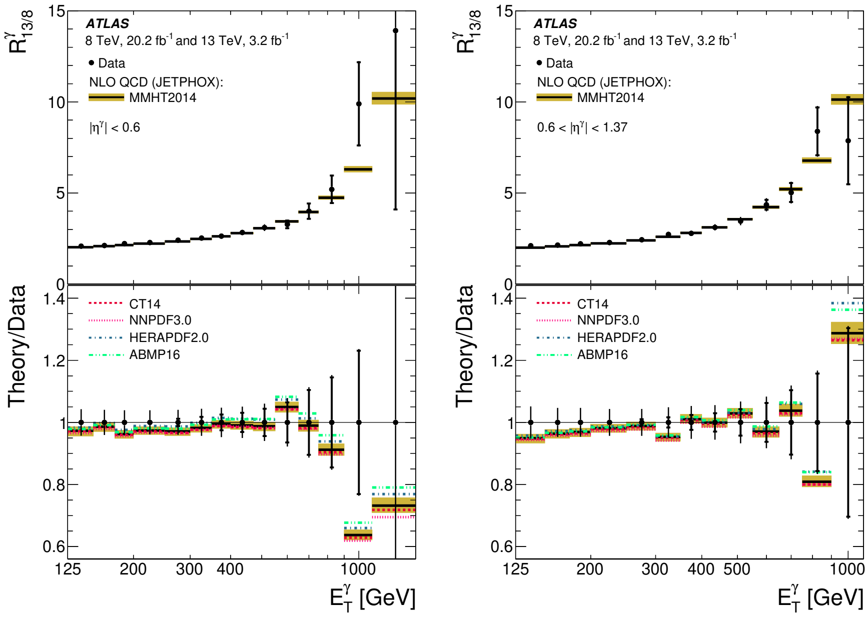


**Figure 1:** The measured $R^{\gamma}_{13/8}$ (dots) as a function of $E^{\gamma}_{\mathrm{T}}$ in different regions of $|\eta^{\gamma}|$ [11]. The NLO QCD predictions from JETPHOX are also shown. The lower part of the figures shows the ratio of the NLO QCD predictions to the measured $R^{\gamma}_{13/8}$ (black lines). The ratios of the NLO QCD predictions based on different PDF sets to the measured $R^{\gamma}_{13/8}$ are also included.

## 3. Measurement of the cross section for isolated-photon plus jet at $\sqrt{s}$ = 13 TeV

The dynamics of isolated-photon production in association with a jet in proton–proton collisions at $\sqrt{s}$ = 13 TeV is studied using a dataset with an integrated luminosity of 3.2 fb$^{-1}$ [13]. The kinematics of the photon plus one-jet is studied via measurements of the cross sections as functions of the $E^{\gamma}_{\mathrm{T}}$ and the leading-jet transverse momentum ($p_{\mathrm{T}}^{\mathrm{jet-lead}}$), whereas the dynamics of the system is studied by measuring the azimuthal angular separation between the leading photon and the leading jet ($\Delta\phi^{\gamma-\mathrm{jet}}$), the invariant mass of the leading photon and the leading jet ($m^{\gamma-\mathrm{jet}}$) and $|\cos\theta^{*}|$. Photons are required to have $E^{\gamma}_{\mathrm{T}} > 125$ GeV. Jets are reconstructed using the anti-kt algorithm with radius parameter R = 0.4 using topological clusters as input and required to have $p_{\mathrm{T}} > 100$ GeV and $|y^{\mathrm{jet}}| < 2.37$. Jets are further calibrated using the method described in Ref. [14]. Jets reconstructed from calorimeter signals not originating from a $pp$ collision are rejected by applying jet-quality criteria [15, 16]. The selected jets and the photon must be separated by $\Delta R > 0.8$. For the measurements of $m^{\gamma-\mathrm{jet}}$ and $|\cos\theta^{*}|$ additional constraints $|\eta^{\gamma} + y^{\mathrm{jet-lead}}| < 2.37$, $|\cos\theta^{*}| < 0.83$ and $m^{\gamma-\mathrm{jet}} > 450$ GeV are applied to remove bias due to the selection requirements on the photon and jet. The dominant sources of uncertainty arise from the jet and photon energy scales and the photon identification. In each case the results are propagated through all steps of the analysis to keep correlations.

The fiducial measured cross section is: $\sigma_{\mathrm{meas}} = 300 \pm 10$ (exp.) $\pm$ 6 (lumi.) pb. The measurement is consistent with the fiducial cross sections predicted by JETPHOX and a multi-leg NLO QCD plus parton-shower Monte Carlo (SHERPA) [17, 18]. Both types of NLO QCD prediction describe the data within the experimental and theoretical uncertainties (see Figure 2), although there is a tendency of the NLO QCD calculations to overestimate the data in the tail of the $p_{\mathrm{T}}^{\mathrm{jet-lead}}$ and $m^{\gamma-\mathrm{jet}}$. For most of the points, the theoretical uncertainties are larger than those of experimental origin. Recently published NNLO pQCD calculations [19] give an excellent description of the measurements with reduced theoretical uncertainties (not shown).

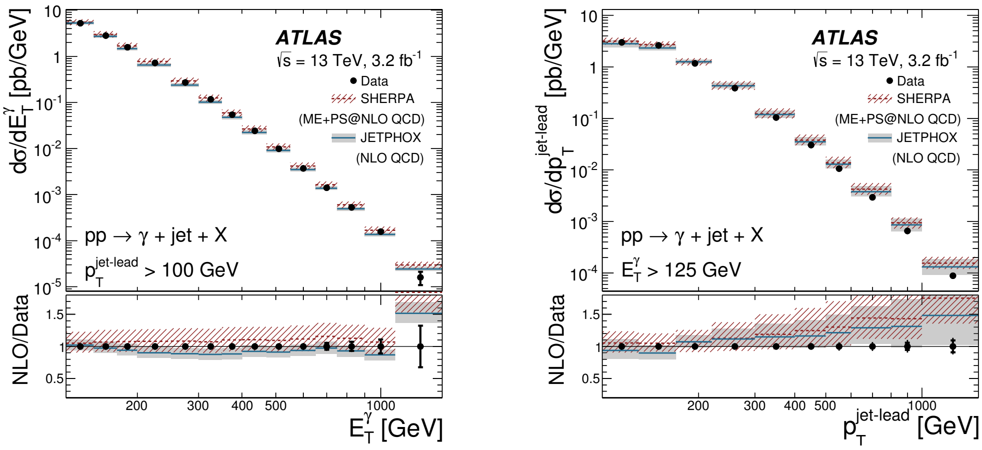


**Figure 2:** Measured cross sections for isolated-photon plus jet production (dots) as functions of $E_{\mathrm{T}}^{\gamma}$ (left plot) and $p_{\mathrm{T}}^{\mathrm{jet-lead}}$ (right plot). For comparison, the multi-leg NLO QCD plus parton shower predictions from SHERPA (dashed lines) and the NLO QCD predictions from JETPHOX corrected for hadronisation and UE effects (solid lines) are also shown. The bottom part of each figure shows the ratios of the predictions to the measured cross section [13].

## 4. Measurement of the inclusive isolated-photon cross section at $\sqrt{s}$ = 13 TeV

The differential cross section for isolated-photon production in $pp$ collisions is measured at $\sqrt{s}$ = 13 TeV using an integrated luminosity of 36.1 fb$^{1}$ [20]. The differential cross section as a function of $E_{\mathrm{T}}^{\gamma}$ is measured in different regions of $|\eta^{\gamma}|$ for $E_{\mathrm{T}}^{\gamma} > 125$ GeV and $|\eta^{\gamma}| < 2.37$, excluding the region 1.37$<|\eta^{\gamma}|<$1.56. In this analysis, the region where the measurement is limited by systematic uncertainties is extended to $E_{T}^{\gamma} \sim$ 1TeV, beyond what was achieved in the previous measurement [2]. The NLO QCD predictions of JETPHOX and SHERPA based on several parameterisations of the PDFs are compared with the measurement. The NNLO QCD prediction of NNLOJET [19], which has significantly reduced uncertainties due to fewer missing higher-order terms, is also confronted with the data. The total systematic uncertainty of the measurements is in the range 3%–17%, depending on $E_{\mathrm{T}}^{\gamma}$ and the $|\eta^{\gamma}|$ region. The dominant sources of uncertainty arise from the photon energy scale, the photon identification efficiency and the integrated luminosity.

The measurement of the inclusive isolated-photon differential cross section as a function of $E_{\mathrm{T}}^{\gamma}$ in different regions of $|\eta^{\gamma}|$ is shown in Figure 3. The NNLO QCD prediction gives an excellent description of the data. The comparison of the NNLO QCD prediction with the measured cross section represents a precise test of the theory at $O(\alpha_{\rm EM}\alpha_S^3)$ in the range of photon transverse energies from 125 GeV up to and beyond 1 TeV. The measurement has the potential to further constrain the PDFs, particularly the gluon density in the proton, within a global QCD fit.

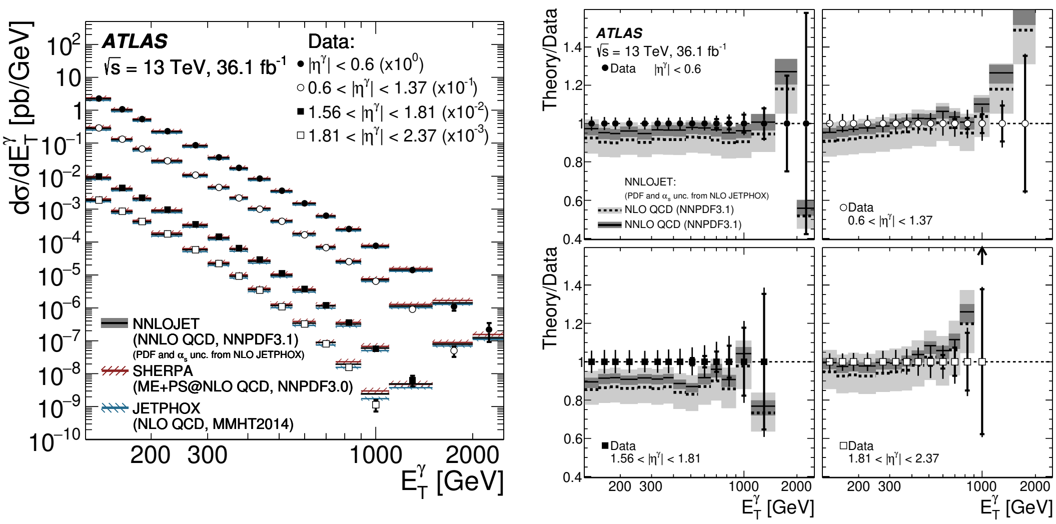


**Figure 3:** Left plot shows the measured differential cross section for isolated-photon production as a function of $E_{\rm T}^{\gamma}$ in different $|\eta^{\gamma}|$ regions. The NLO pQCD prediction from JETPHOX, the ME+PS@NLO QCD prediction from SHERPA and the NNLO QCD prediction from NNLOJET are also shown. In addition, the ratio of the NNLO (NLO) QCD prediction of NNLOJET to the measured differential cross sections is shown on the right plot [20].

## 5. Summary

The measurement of the ratio of the cross sections for inclusive isolated-photon production at $\sqrt{s}$ = 13 TeV and 8 TeV, of the isolated-photon plus jet cross sections at $\sqrt{s}$ = 13 TeV and of the isolated-photon cross section at $\sqrt{s}$ = 13 TeV by the ATLAS experiment at the LHC are presented. The measurements are compared to NLO QCD calculations made by JETPHOX, the multi-leg NLO QCD plus parton-shower predictions from SHERPA and the NNLO QCD calculations from NNLOJET. Both types of NLO QCD prediction describe the data within the experimental and theoretical uncertainties, although they show a tendency to overestimate the data in the photon plus jet measurements in the tail of $d\sigma/dp_{\rm T}^{\rm jet-lead}$ and $d\sigma/dm^{\gamma-\rm jet}$ distributions. Comparison of the NNLO QCD predictions to data shows excellent agreement. These measurements have the potential to further constrain the PDFs, particularly the gluon density in the proton, within a global QCD fit.

## References


[1] ATLAS Collaboration, *Measurement of the inclusive isolated prompt photon cross section in pp collisions at* $\sqrt{s} = 8\,$TeV *with the ATLAS detector*, *JHEP* **08** (2016) 005 [arXiv:1605.03495].

[2] ATLAS Collaboration, *Measurement of the cross section for inclusive isolated-photon production in pp collisions at* $\sqrt{s} = 13\,$TeV *using the ATLAS detector*, *Phys. Lett. B* **770** (2017) 473 [arXiv:1701.06882].

[3] A.V. Lipatov and M.A. Malyshev, *Reconsideration of the inclusive prompt photon production at the LHC with kT-factorization*, *Phys. Rev. D* **94** (2016) 034020 [arXiv:1606.02696].

[4] M.D. Schwartz, *Precision direct photon spectra at high energy and comparison to the 8 TeV ATLAS data*, *JHEP* **1609** (2016) 005 [arXiv:1606.02313].

[5] P. Aurenche, R. Baier, M. Fontannaz, J.F. Owens and M. Werlen, *The Gluon Contents of the Nucleon Probed with Real and Virtual Photons*, *Phys. Rev. D* **39** (1989) 3275.

[6] ATLAS Collaboration, *The ATLAS Experiment at the CERN Large Hadron Collider*, *JINST* **3** (2008) S08003.

[7] ATLAS Collaboration, *Electron and photon energy calibration with the ATLAS detector using LHC Run 1 data*, *Eur. Phys. J. C* **74** (2014) 3071 [arXiv:1407.5063].

[8] ATLAS Collaboration, *Measurement of the photon identification efficiencies with the ATLAS detector using LHC Run 2 data collected in 2015 and 2016*, *Eur. Phys. J. C* **79** (2019) 205 [arXiv:1810.05087].

[9] M. Cacciari, G. P. Salam and S. Sapeta, *On the characterisation of the underlying event*, *JHEP* **04** (2010) 065 [arXiv:0912.4926].

[10] ATLAS Collaboration, *Measurement of the inclusive isolated prompt photons cross section in pp collisions at* $\sqrt{s} = 7\,\mathrm{TeV}$ *with the ATLAS detector using* $4.6\,\mathrm{fb}^{-1}$, *Phys. Rev. D* **89** (2014) 052004 [arXiv:1311.1440].

[11] ATLAS Collaboration, *Measurement of the ratio of cross sections for inclusive isolated-photon production in pp collisions at* $\sqrt{s} = 13$ *and* $8\,\mathrm{TeV}$ *with the ATLAS detector*, *JHEP* **04** (2019) 093 [arXiv:1901.10075].

[12] S. Catani, M. Fontannaz, J. Ph. Guillet and E. Pilon, *Cross section of isolated prompt photons in hadron-hadron collisions*, *JHEP* **05** (2002) 028 [arXiv:0204023].

[13] ATLAS Collaboration, *Measurement of the cross section for isolated-photon plus jet production in pp collisions at* $\sqrt{s} = 13\,\mathrm{TeV}$ *using the ATLAS detector*, *Phys. Lett. B* **780** (2018) 578 [arXiv:1801.00112].

[14] ATLAS Collaboration, *Jet energy scale measurements and their systematic uncertainties in proton–proton collisions at* $\sqrt{s} = 13\,\mathrm{TeV}$ *with the ATLAS detector*, *Phys. Rev. D* **96** (2017) 072002 [arXiv:1703.09665].

[15] ATLAS Collaboration, *Jet energy measurement and its systematic uncertainty in proton–proton collisions at* $\sqrt{s} = 7\,\mathrm{TeV}$ *with the ATLAS detector*, *Eur. Phys. J. C* **75** (2015) 17 [arXiv:1406.0076].

[16] ATLAS Collaboration, *Jet energy measurement with the ATLAS detector in proton–proton collisions at* $\sqrt{s} = 7\,\mathrm{TeV}$, *Eur. Phys. J. C* **73** (2013) 2304 [arXiv:1112.6426].

[17] T. Gleisberg et al., *Event generation with SHERPA 1.1*, *JHEP* **02** (2009) 007 [arXiv:0811.4622].

[18] E. Bothmann et al., *Event Generation with Sherpa 2.2*, *SciPost Phys.* **07** (2019) 34 [arXiv:1905.09127].

[19] Xuan Chen, Thomas Gehrmann, Nigel Glover, Marius Höfer, Alexander Huss, *Isolated photon and photon+jet production at NNLO QCD accuracy*, arXiv:1904.01044.

[20] ATLAS Collaboration, *Measurement of the inclusive isolated-photon cross section in pp collisions at* $\sqrt{s} = 13\,\mathrm{TeV}$ *using* $36\ \mathrm{fb}^{-1}$ *of ATLAS data*, arXiv:1908.02746.




PoS(EPS-HEP2019)648